

Investigation of the Interactions between Ligand-Stabilized Gold Nanoparticles and Polyelectrolyte Multilayer Films

Jinhan Cho[†] and Frank Caruso*

Centre for Nanoscience and Nanotechnology, Department of Chemical and Biomolecular Engineering,
The University of Melbourne, Victoria 3010, Australia

Received May 9, 2005. Revised Manuscript Received June 23, 2005

We examine the interactions between gold nanoparticles stabilized by the 4-(dimethylamino)pyridine (DMAP–Au_{NP}) and various polyelectrolytes (PEs), both in solution and in layer-by-layer (LbL) assembled multilayer films. UV–vis spectrophotometry studies showed that the plasmon absorption band of the DMAP–Au_{NP} in solution red-shifts and broadens in the presence of poly(sodium 4-styrenesulfonate) (PSS), poly(allylamine hydrochloride) (PAH), or poly(ethyleneimine) (PEI). This suggests that the polyanion PSS electrostatically associates with the nanoparticles, while PAH and PEI bond through the amine functionalities, despite having the same charge as the nanoparticles. In contrast, the addition of poly(diallyldimethylammonium chloride) (PDADMAC) to a DMAP–Au_{NP} dispersion has no influence on either the peak position or shape of the absorption spectrum of the nanoparticles, indicating no interaction. PE/nanoparticle hybrid films were assembled by a single-step adsorption of the DMAP–Au_{NP} into preassembled LbL PE multilayer films. The interactions between the DMAP–Au_{NP} and the multilayer films were investigated by UV–vis spectrophotometry, quartz crystal microgravimetry, and surface plasmon resonance spectroscopy. These experiments revealed that PAH/PSS films have a highly uniform and dense DMAP–Au_{NP} coverage, which is attributed to the bonds formed between the nanoparticles and PAH and PSS in the films. Additionally, the DMAP–Au_{NP} adsorbed amount and the nanoparticle–nanoparticle interactions (and hence film optical properties) can be controlled by the number of preassembled PAH/PSS bilayers. In contrast, for PDADMAC/PSS films only a sparse and nonuniform DMAP–Au_{NP} coating is obtained, and an irregular trend between PE bilayer number and DMAP–Au_{NP} adsorbed amount was observed. The results obtained indicate that the combined interactions originating from PAH and PSS with DMAP–Au_{NP} facilitate the preparation of stable nanoparticle/PE thin films with tailored optical properties. Such films may be exploited in diverse areas, including electrochemical sensing, colloidal crystals, and controlled delivery.

Introduction

Nanostructured films based on metal nanoparticle building blocks, formed on either planar or colloidal substrates, have attracted widespread interest due to their unique optical, electrical, or magnetic properties.^{1–15} The functional proper-

ties of such films are mainly governed by the size,^{16,17} shape,¹⁸ and distribution^{1,4,7,11} of the metal nanoparticles as well as the properties of the medium surrounding the nanoparticles.¹⁹ Of particular interest has been the formation of thin films with a high density of metal nanoparticles, which is often desired for catalysis and electronic applications.² Although films comprising close-packed metal nanoparticles can be prepared via self-assembly of nanoparticles from organic media onto solid supports,^{20–24} the generation

* To whom correspondence should be addressed. Fax: +61 3 8344 4153. E-mail: fcaruso@unimelb.edu.au.

[†] Present address: Information & Electronic Materials, LG Chem./Research Park, Daejeon, 305-380, Korea.

- (1) Oldenberg, S. J.; Averitt, R. D.; Westcott, S. L.; Halas, N. J. *Chem. Phys. Lett.* **1998**, *288*, 243.
- (2) Oldenberg, S. J.; Westcott, S. L.; Averitt, R. D.; Halas, N. J. *J. Chem. Phys.* **1999**, *111*, 4729.
- (3) Oldenberg, S. J.; Jackson, J. B.; Westcott, S. L.; Halas, N. J. *Appl. Phys. Lett.* **1999**, *75*, 2897.
- (4) Collier, C. P.; Saykally, R. J.; Shiang, J. J.; Henrichs, S. E.; Heath, J. R. *Science* **1997**, *277*, 1978.
- (5) Henrichs, S.; Collier, C. P.; Saykally, R. J.; Shen, Y. R.; Heath, J. R. *J. Am. Chem. Soc.* **2000**, *122*, 4077.
- (6) Wang, D.; Salgueirião-Maceira, V.; Liz-Marzán, L. M.; Caruso, F. *Adv. Mater.* **2002**, *14*, 908.
- (7) Caruso, F.; Spasova, M.; Salgueirião-Maceira, V.; Liz-Marzán, L. M. *Adv. Mater.* **2001**, *13*, 1090.
- (8) Cassagneau, T.; Caruso, F. *Adv. Mater.* **2002**, *14*, 732.
- (9) Chandrasekharan, N.; Kamat, P. *Nano Lett.* **2001**, *1*, 67.
- (10) Doron, A.; Katz, E.; Willner, I. *Langmuir* **1995**, *11*, 1313.
- (11) Ung, T.; Liz-Marzán, L. M.; Mulvaney, P. *J. Phys. Chem. B* **2001**, *105*, 3441.
- (12) Kepley, L. J.; Sackett, D. D.; Bell, C. M.; Mallouk, T. E. *Thin Solid Films* **1992**, *208*, 132.

- (13) Katz, H. E.; Schilling, M. L. *Chem. Mater.* **1993**, *5*, 1162.
- (14) *Nanoparticles and Nanostructured Films. Preparation, Characterization and Applications*; Fendler, J. H., Ed.; WILEY-VCH: Weinheim, 1998.
- (15) Hyeon, T.; Lee, S. S.; Park, J.; Chung, Y.; Na, H. B. *J. Am. Chem. Soc.* **2001**, *123*, 12798.
- (16) Teranishi, T.; Hasegawa, S.; Shimizu, T.; Miyake, M. *Adv. Mater.* **2001**, *13*, 1699.
- (17) Link, S.; El-Sayed, M. A. *J. Phys. Chem. B* **1999**, *103*, 4212.
- (18) Link, S.; Burda, C.; Mohamed, M. B.; Nikoobakht, B.; El-Sayed, M. A. *J. Phys. Chem. A* **1999**, *103*, 1165.
- (19) Schmitt, J.; Mächtle, P.; Eck, D.; Möhwald, H.; Helm, C. A. *Langmuir* **1999**, *15*, 3256.
- (20) Collier, C. P.; Vossmeier, T.; Heath, J. R. *Annu. Rev. Mater. Sci.* **1998**, *49*, 371.
- (21) Wang, Z. L. *Adv. Mater.* **1998**, *10*, 13.
- (22) Kiely, C. J.; Fink, J.; Zheng, J. G.; Brust, M.; Bethell, D.; Schiffrin, D. J. *Adv. Mater.* **2000**, *12*, 640.
- (23) Brown, L. O.; Hutchison, J. E. *J. Phys. Chem. B* **2001**, *105*, 8911.
- (24) Thomas, K. G.; Zajicek, J.; Kamat, P. V. *Langmuir* **2002**, *18*, 3722.

of dense metal nanoparticle films from aqueous nanoparticle dispersions is often difficult,^{25–32} with nanoparticle surface coverages of less than about 30% commonly achieved.³³ The nanoparticle loading on surfaces can be increased by using additional linker molecules to bind extra nanoparticles to the surface.^{25,26,34} Alternatively, as we recently demonstrated, thin films comprising a dense packing of gold nanoparticles can be prepared by the adsorption of 4-(dimethylamino)pyridine gold nanoparticles (DMAP–Au_{NP}) into preformed polyelectrolyte (PE) films.³⁵ The formation of dense nanoparticle films was attributed to the reversible binding nature of the DMAP ligand and the nature of the PE films employed (poly(sodium 4-styrenesulfonate) (PSS) and poly(allylamine hydrochloride) (PAH)), which act as matrixes for nanoparticle adsorption.^{35–41} We recently reported that PAH/PSS multilayer films loaded with DMAP–Au_{NP} can be used as coatings on colloids to modulate the optical properties of colloidal crystals,^{36–38} as electrochemical sensors,³⁹ and as nanostructured optically addressable capsules that can be irradiated with near-infrared light for the release of (bio)-macromolecules.^{40,41} The ability to construct nanoparticle-based thin films with controlled and tailored properties, as well as their ultimate application, is dependent on a fundamental understanding of the interactions involved.

Herein, we report on the interactions between DMAP–Au_{NP} and PEs, both in the form of single components in solution and in the adsorbed state as multicomponent thin LbL multilayer films. We investigate positively charged PEs (i.e., PAH, poly(ethyleneimine) (PEI), and poly(diallyldimethylammonium chloride) (PDADMAC), which contain primary amine, mixed amine (primary, secondary and tertiary),⁴² and quaternary ammonium groups, respectively) and the polyanion PSS. The structures of the PEs and the DMAP–Au_{NP} used in this study are shown in Figure 1. For the LbL assembled thin films, we chose PAH/PSS and

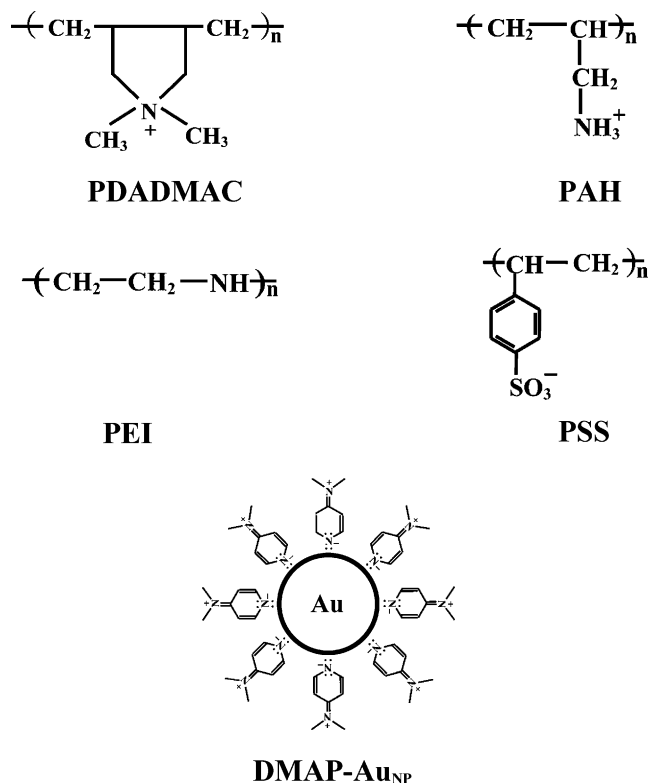


Figure 1. Chemical structures of the PEs used in this study and a schematic of the DMAP–Au_{NP}.

PDADMAC/PSS films, as these are commonly studied systems. Negatively charged PSS was employed as an outermost layer for films in all cases because PSS electrostatically interacts with the positively charged DMAP–Au_{NP} and has a fixed charge density at the pH (10.5) of the DMAP–Au_{NP} deposition solution. Furthermore, we explore the infiltration depth of the nanoparticles in multilayer films composed of DMAP–Au_{NP}. The current study into the adsorption properties of DMAP–Au_{NP} onto PE multilayer films is required for advances to be made in tailoring properties of these films for applications in sensing, optics, catalysis, and controlled delivery.

Experimental Section

Materials. PSS ($M_w = 70\,000$), PAH ($M_w = 70\,000$), PDADMAC ($M_w = 200\,000$ to $\sim 350\,000$), and PEI ($M_w = 25\,000$) were used as received from Aldrich. PEI is a highly branched polymer with a distribution of primary, secondary, and tertiary amine groups.⁴² The DMAP–Au_{NP} dispersion was synthesized as reported previously.⁴³ The DMAP–Au_{NP} dispersed in water have a diameter of ~ 6 nm and display a surface plasmon band maximum (λ_{max}) at 518 nm. Quartz substrates were purchased from Hellma Optik GmbH (Jena, Germany), and quartz crystal microbalance (QCM) electrodes were obtained from Kyushu Dentsu (Nagasaki, Japan). The quartz slides and silicon wafers were cleaned by treatment with Piranha solution (sulfuric acid/hydrogen peroxide = 70/30 v/v %) (**Caution!** Piranha solution is highly corrosive. Extreme care should be taken when handling Piranha solution, and only small quantities should be prepared.) and subsequently negatively charged by

- (25) Musick, M. D.; Keating, C. D.; Keefe, M. H.; Natan, M. J. *Chem. Mater.* **1997**, *9*, 1499.
 (26) Musick, M. D.; Keating, C. D.; Lyon, L. A.; Botsko, S. L.; Pena, D. J.; Holliday, W. D.; McEvoy, T. M.; Richardson, J. N.; Natan, M. J. *Chem. Mater.* **2000**, *12*, 2869.
 (27) Grabar, K. C.; Allison, K. J.; Baker, B. E.; Bright, R. M.; Brown, K. R.; Freeman, R. G.; Fox, A. P.; Keating, C. D.; Musick, M. D.; Natan, M. J. *Langmuir* **1996**, *12*, 2353.
 (28) Dokoutchaev, A.; James, J. T.; Koene, S. C.; Pathak, S.; Prakash, G. K. S.; Thompson, M. E. *Chem. Mater.* **1999**, *11*, 2389.
 (29) Pathak, S.; Greci, M. T.; Kwong, R. C.; Mercado, K.; Prakash, G. K. S.; Olah, G. A.; Thompson, M. E. *Chem. Mater.* **2000**, *12*, 1985.
 (30) Ji, T.; Lirtsman, V. G.; Avny, Y.; Davidov, D. *Adv. Mater.* **2001**, *13*, 1253.
 (31) Kooij, E. S.; Wormeester, H.; Brouwer, E. A. M.; Vroonhoven, E. V.; Silfhout, A. V.; Poelsema, B. *Langmuir* **2002**, *18*, 4401.
 (32) Fu, Y.; Xu, H.; Bai, S.; Qiu, D.; Sun, J.; Wang, Z.; Zhang, X. *Macromol. Rapid Commun.* **2002**, *23*, 256.
 (33) Schmitt, J.; Decher, G.; Dressick, W. J.; Brandow, S. L.; Geer, R. E.; Shashidhar, R.; Calvert, J. M. *Adv. Mater.* **1997**, *9*, 61.
 (34) Wuelfing, W. P.; Zamborini, F. P.; Templeton, A. C.; Wen, X.; Yoon, H.; Murray, R. W. *Chem. Mater.* **2001**, *13*, 87.
 (35) Gittins, D. I.; Susha, A. S.; Schoeler, B.; Caruso, F. *Adv. Mater.* **2002**, *14*, 508.
 (36) Liang, Z.; Susha, A. S.; Caruso, F. *Adv. Mater.* **2002**, *14*, 1160.
 (37) Liang, Z.; Susha, A.; Caruso, F. *Chem. Mater.* **2003**, *15*, 3176.
 (38) Miclea, P. T.; Susha, A. S.; Liang, Z.; Caruso, F.; Sotomayor Torres, C. M.; Romanov, S. G. *Appl. Phys. Lett.* **2004**, *84*, 3960.
 (39) Yu, A.; Liang, Z.; Cho, J.; Caruso, F. *Nano Lett.* **2003**, *3*, 1203.
 (40) Radt, B.; Smith, T. A.; Caruso, F. *Adv. Mater.* **2004**, *16*, 2184.
 (41) Angelatos, A. S.; Radt, B.; Caruso, F. *J. Phys. Chem. B* **2005**, *109*, 3071.

- (42) (a) Chance, J. J.; Purdy, W. C. *Langmuir* **1997**, *13*, 4487. (b) Bahulekar, R.; Ayyangar, N. R.; Ponrathnam, S. *Enzyme Microb. Technol.* **1991**, *13* (11), 858.
 (43) Gittins, D. I.; Caruso, F. *Angew. Chem., Int. Ed.* **2001**, *40*, 3001.

heating at 70 °C for 20 min in a 5:1:1 vol% mixture of water, hydrogen peroxide, and 29% ammonia solution. Sulfate-stabilized polystyrene (PS) spheres (diameter of 640 nm) were purchased from Microparticles GmbH. Water from a Millipore purification system with a resistivity greater than 18.2 MΩ cm was used for deposition and rinsing solutions in all experiments

Interaction between PEs in Solution and DMAP–Au_{NP}. UV–vis spectra were measured for DMAP–Au_{NP} dispersions containing different amounts of PEs. PSS, PEI, PAH, or PDADMAC were added to 100 mL of diluted DMAP–Au_{NP} dispersions with a final concentration of 5×10^{13} particles mL⁻¹ at pH 10.5 (i.e., 5 mL of the as-prepared DMAP–Au_{NP} dispersion (1×10^{15} particles mL⁻¹) was added to 95 mL of deionized water), after which the dispersion was stirred for about 5 min, and then the UV–vis spectrum recorded.

Preparation of PE/DMAP–Au_{NP} Films. The concentration of PE solutions used for all experiments was 1 mg mL⁻¹. All of the PE solutions contained 0.5 M NaCl. The quartz (for UV–vis) and gold (QCM, surface plasmon resonance (SPR)) substrates were first dipped for 20 min in the cationic PE (PAH, PDADMAC or PEI) solution, washed three times by dipping in water for 2 min, followed by drying with a gentle stream of nitrogen. Negatively charged PSS layers were subsequently deposited onto the positively charged substrates by using the same washing and drying procedure as described above. The outermost layers of the PE multilayer films fabricated were always PSS, as the DMAP–Au_{NP} bear a cationic charge. This facilitates nanoparticle deposition onto the PE multilayer films. The PE multilayer films were immersed in a DMAP–Au_{NP} solution for 60 min. Two different sample series were prepared using the different cationic PE layers: (PAH/PSS)_n/DMAP–Au_{NP} and (PDADMAC/PSS)_n/DMAP–Au_{NP}. PE multilayer-coated PS particles were prepared as follows: 100 μL of a concentrated dispersion (6.4 wt %) of negatively charged 640 nm PS particles was diluted to 0.5 mL with deionized water. Then, 0.5 mL of PAH or PDADMAC (1 mg mL⁻¹ containing 0.5 M NaCl) was added, and after 20 min the excess PE was removed by three repeated centrifugation (7000 g, 5 min)/wash cycles. PSS (1 mg mL⁻¹ containing 0.5 M NaCl) was then deposited onto the PAH (or PDADMAC)-coated PS particles using the same conditions. The above process was repeated until four PAH/PSS or PDADMAC/PSS bilayers were deposited. The PE/DMAP–Au_{NP}-coated PS particles were prepared by adding 0.5 mL of the as-prepared DMAP–Au_{NP} dispersion to the PE-coated PS particles and allowing 60 min for adsorption. The PE/DMAP–Au_{NP}-coated particles were then purified by three centrifugation/water wash cycles.

UV–Vis Spectrophotometry. UV–vis spectra were taken with a HP5453 UV–vis spectrophotometer.

QCM Measurements. A QCM device was used to investigate the mass of material deposited after each adsorption step. The resonance frequency of the QCM electrodes of area 1.59×10^{-5} m² was ca. 9 MHz. The adsorbed mass of the DMAP–Au_{NP}, m , can be calculated from the change in QCM frequency, ΔF , according to the Sauerbrey equation:⁴⁴ ΔF (Hz) = $-(1.83 \times 10^4)\Delta m_A$, where m_A is the mass change per quartz crystal unit area, in g m⁻².⁴⁵

Ellipsometry. The thicknesses of PE multilayer films on silicon wafers were measured by ellipsometry (Multiskop from Optrel GmbH). The refractive index was allowed to vary in fitting the ellipsometric data using an iterative process.

SPR Measurements. A full plasmon resonance curve (reflectivity versus internal angle) for the gold/aqueous DMAP solution

(0.1 M) system was first measured. The PE multilayers were deposited onto the gold substrates following the procedure described earlier. The full SPR curves for measuring the thickness of the adsorbed PE multilayers in DMAP solution were then recorded. The SPR curves obtained were fitted to Fresnel theory assuming the idealized layer model. In the fitting procedure, the real (ϵ_r) and imaginary (ϵ_i) components of the relative permittivity of the layer were kept fixed (and hence refractive index, since $\epsilon_r = n^2$, where n is the refractive index), and the thickness (d) was extracted.⁴⁶ Details concerning the fitting procedure can be found in earlier work.⁴⁵ Fits to Fresnel theory are relatively insensitive to minor variations in the refractive index of the dielectric material. In our experiments, it is estimated that these variations account for deviations of up to 10% in the calculated thickness of the films.

Results and Discussion

Interaction of DMAP–Au_{NP} and PEs in Solution. First, we investigated the interactions between four different PEs (i.e., PSS, PEI, PAH, and PDADMAC) and the DMAP–Au_{NP} in aqueous solution. Figure 2 displays the change in plasmon absorption spectra of the DMAP–Au_{NP} due to interactions with the various PEs. As shown in Figure 2a, the absorption spectra of the DMAP–Au_{NP} is broadened and red-shifted with increasing concentration of PSS (from 0 to 0.6 mg mL⁻¹) added to the DMAP–Au_{NP} dispersion. This broadening and red-shift of absorption spectra are mainly due to a reduced nanoparticle–nanoparticle distance^{47,48} and a change in the refractive index¹⁹ as a result of the PSS adsorbed onto the DMAP–Au_{NP}. This suggests electrostatic interaction between the DMAP–Au_{NP} and PSS. It may be also possible that displacement of some DMAP from the Au_{NP} surface occurs upon PSS adsorption. Despite the DMAP ligands stabilizing the Au_{NP}, the DMAP ligands can be reversibly adsorbed/desorbed from the Au_{NP} surface, as previously reported.^{35,43} For PEI, which has coexisting primary, secondary, and tertiary amine groups,⁴² bonding to the gold nanoparticle surface occurs through the amine functionalities.⁴⁹ It has been reported that amines bind to gold nanoparticles through the amine functionality via a weak covalent bond.^{49a,d} Accordingly, the addition of PEI to a DMAP–Au_{NP} dispersion causes a red-shift of the plasmon absorption peak as well as peak broadening (Figure 2b). The high affinity existing between the DMAP–Au_{NP} and of PEI can also be extended to PAH, which contains uncharged amine groups (–NH₂) at the pH of the DMAP–Au_{NP} dispersion (10.5) (the pK_a of PAH in bulk solution is ~8–9).⁵⁰ As a result, PAH can bond to the nanoparticle surface.⁴⁹ Furthermore, upon further increasing the added amount of

(46) Geddes, N. J.; Martin, A. S.; Caruso, F.; Urquhart, R. S.; Furlong, D. N.; Sambles, J. R.; Than, K. A.; Edgar, J. A. *J. Immunol. Methods* **1994**, *175*, 149.

(47) Mirkin, C. A.; Letsinger, R. L.; Mucic, R. C.; Storhoff, J. J. *Nature* **1996**, *382*, 607.

(48) Brust, M.; Bethell, D.; Kiely, C. J.; Schiffrin, D. J. *Langmuir* **1998**, *14*, 5425.

(49) (a) Leff, D. V.; Brandt, L.; Heath, J. R. *Langmuir* **1996**, *12*, 4723. (b) Chen, X. Y.; Li, J. R.; Jiang, L. *Nanotechnology* **2000**, *11*, 108. (c) Brown, L. O.; Hutchison, J. E. *J. Am. Chem. Soc.* **1999**, *121*, 882. (d) Mukhopadhyay, K.; Phadtare, S.; Vinod, V. P.; Kumar, A.; Rao, M.; Chaudhari, R. V.; Sastry, M. *Langmuir* **2003**, *19*, 3858. (e) Selvakannan, P. R.; Mandal, S.; Pasricha, R.; Adyantaya, S. D.; Sastry, M. *Chem. Commun.* **2002**, 1334.

(50) Choi, J.; Rubner, M. F. *Macromolecules* **2005**, *38*, 116.

(44) Sauerbrey, G. *Z. Phys.* **1959**, *155*, 206.

(45) Caruso, F.; Niikura, K.; Furlong, D.; Okahata, Y. *Langmuir* **1997**, *13*, 3422.

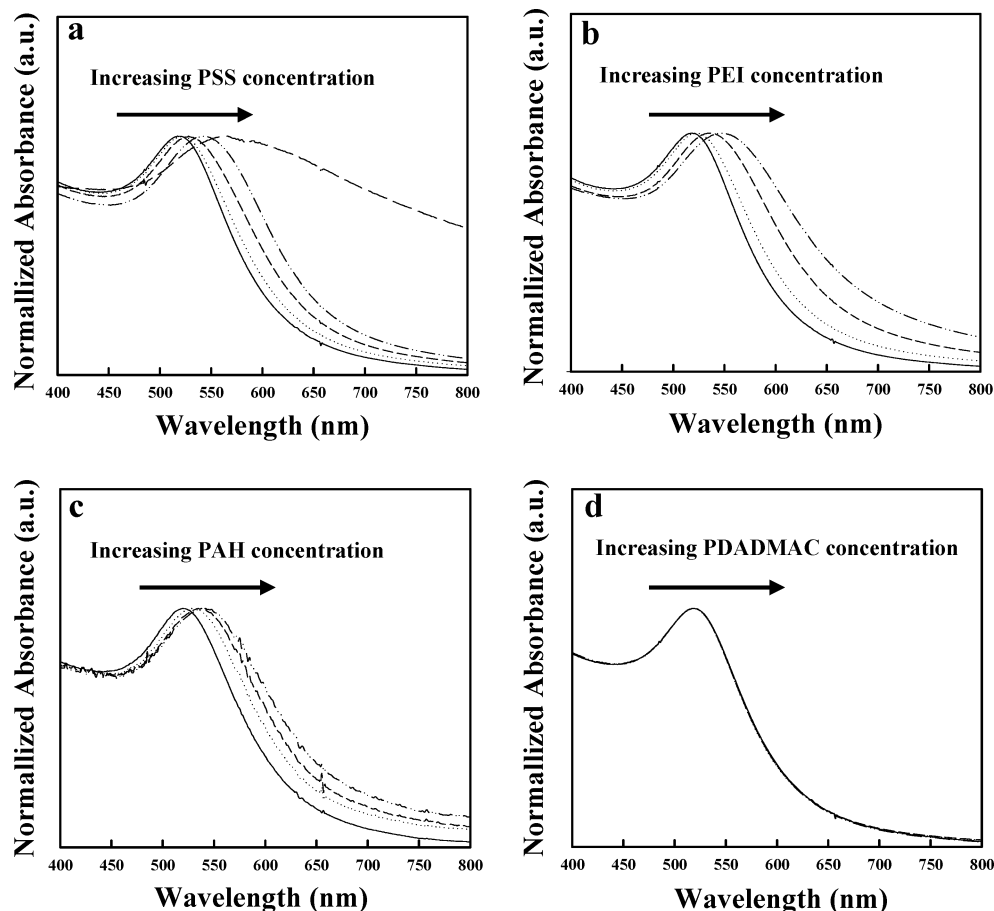


Figure 2. UV-vis absorption spectra measured for DMAP-Au_{NP} dispersions (5×10^{13} particles mL⁻¹, pH = 10.5) with increasing concentrations of (a) PSS (0, 0.01, 0.03, 0.1, and 0.6 mg mL⁻¹), (b) PEI (0, 0.2, 0.4, and 0.6 mg mL⁻¹), and (c) PAH (0, 0.2, 0.4, and 2 mg mL⁻¹). (d) PDADMAC (0, 5, 10, and 20 mg mL⁻¹). PDADMAC had no effect on the position of the DMAP-Au_{NP} absorbance peak.

PE (PAH, PEI, or PSS) to 20 mg mL⁻¹ in the DMAP-Au_{NP} dispersion, the plasmon absorption peak further red-shifts and broadens, and the nanoparticles precipitate within relatively short times (minutes) (see Figure 2a). On the contrary, the successive addition of PDADMAC (from 0 to 20 mg mL⁻¹), which contains a quaternary ammonium group, to the DMAP-Au_{NP} dispersion had no effect on the position and shape of the nanoparticle plasmon absorption peak, suggesting no interaction between the DMAP-Au_{NP} and PDADMAC (Figure 2d). We note that lower concentrations of PSS compared with PEI and PAH are required to induce a significant red-shift and broadening of the nanoparticle absorption spectrum. The above results demonstrate that the DMAP-Au_{NP} associate with typical PEs (with the exception of PDADMAC) employed to assemble LbL PE multilayer films.

Adsorption of DMAP-Au_{NP} onto PE Multilayer Films.

Figure 3 indicates the change in the UV-vis spectra of DMAP-Au_{NP} deposited onto (PAH/PSS)₄ multilayers as a function of adsorption time. The plasmon absorption peak (λ_{\max}) red-shifts from 583 ($t_{\text{ads}} = 5$ min) to 603 nm during the first 10 min of adsorption and then blue-shifts from 603 to 593 nm with increasing adsorption time from 10 to 2400 min. In addition, the absorbance measured at λ_{\max} significantly increased within the first 60 min, after which only a further increase of $\sim 20\%$ and essentially saturation of the film absorbance was observed (Figure 3 inset). Despite the

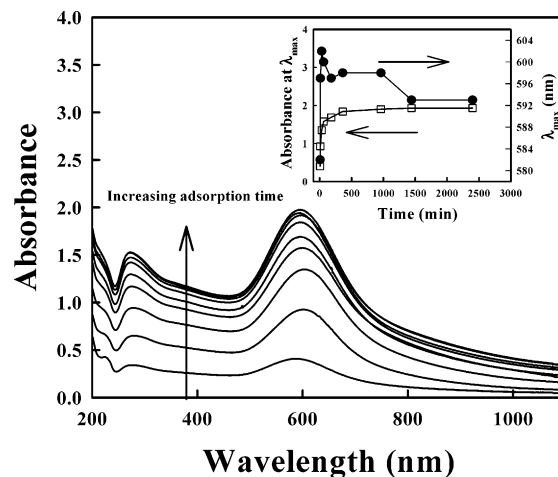


Figure 3. UV-vis absorption spectra of (PAH/PSS)₄ multilayer films as a function of DMAP-Au_{NP} adsorption time. Spectra (from bottom to top): 5, 10, 40, 60, 120, 300, 900, 1400, and 2400 min. The inset shows the film absorbance at λ_{\max} (squares) and the λ_{\max} position (circles) as a function of DMAP-Au_{NP} adsorption time.

fact that there is a shift in λ_{\max} , and hence the film absorbance is not directly proportional to the amount of DMAP-Au_{NP} adsorbed, the red-shift in the absorption peak of the film in the first 10 min reflects an increase in the packing density of DMAP-Au_{NP} in the film. Furthermore, for longer adsorption times, the blue-shift accompanying the absorbance increase indicates an increase in nanoparticle separation (i.e., decreased interaction) in the films with

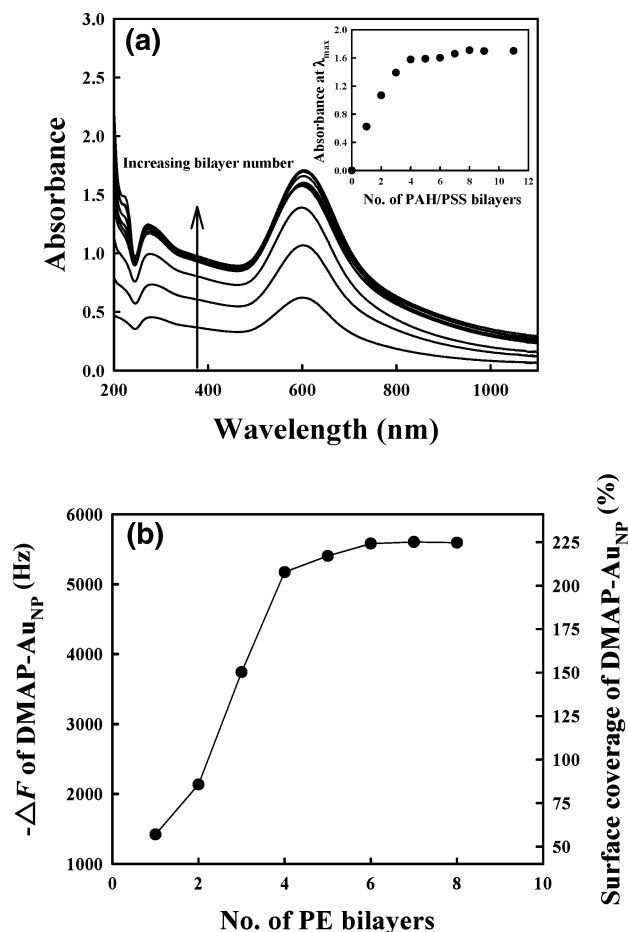


Figure 4. (a) UV-vis absorption spectra of DMAP-AuNP adsorbed onto (PAH/PSS)_n multilayer films with increasing bilayer number (*n*). Spectra (from bottom to top): *n* = 1 to 11. DMAP-AuNP adsorption time = 60 min. Each point in the inset represents the absorbance measured at λ_{max} as a function of PAH/PSS bilayer number. (b) QCM frequency change and surface coverage (%) of DMAP-AuNP vs (PAH/PSS) bilayer number (here, the first layer deposited onto the gold QCM electrodes was PEI instead of PAH). The surface coverage of the DMAP-AuNP was calculated from the QCM frequency changes.

continued infiltration and loading of DMAP-AuNP into the PAH/PSS multilayer films. This suggests film rearrangement and perhaps even film swelling at long DMAP-AuNP adsorption times, possibly caused by the 0.1 M DMAP present in the nanoparticle dispersion (to be discussed later).

We next examined the adsorption of DMAP-AuNP in the (PAH/PSS)_n multilayer films with increasing bilayer number (*n*). In this case, the PAH/PSS thickness per bilayer (before the deposition of DMAP-AuNP) was about 3.4 nm (measured from ellipsometry) and the adsorption time for the deposition of DMAP-AuNP onto (PAH/PSS)_n films was 60 min. As shown in Figure 4a, saturation in the absorbance of DMAP-AuNP is achieved for four bilayer (*n* = 4) PAH/PSS films at a constant adsorption time. Similar saturation trends have been observed for the binding of fluorescent dye molecules to PE multilayer films,⁵¹ and suggest that only a constant thickness of the outermost region of the PAH/PSS film is responsible for DMAP-AuNP binding. Figure 4a also shows that increasing the bilayer number of the PAH/PSS films from 1 to 11 has no evident effect on the position of the

plasmon absorption peak, which is centered at 600 (± 2) nm. In view of particle-particle interactions, this suggests that DMAP-AuNP adsorbed onto (PAH/PSS)_n films are separated by a uniform distance and that the distribution of the nanoparticles in the PAH/PSS films is constant with different film thicknesses. However, the amount of DMAP-AuNP adsorbed on the PAH/PSS films increases with increasing bilayer number from 1 to 4. In summary, the results in Figures 3 and 4a show that both the adsorption time and the PE bilayer number significantly influence the adsorbed amount of DMAP-AuNP and that the nanoparticle-nanoparticle distance is principally determined by the adsorption time.

QCM measurements were conducted to measure the adsorbed amount of DMAP-AuNP in the PAH/PSS multilayer films. In this case, we employed PEI instead of PAH for the first PE layer deposited onto the QCM gold electrodes because the amine groups of PEI have a high affinity with gold.^{52,53} Figure 4b shows that the frequency changes, $-\Delta F$, of adsorbed DMAP-AuNP with increasing PAH/PSS bilayer number follows the same trend as the absorbance data (Figure 4a inset). The surface coverage of DMAP-AuNP increases regularly with increasing PE bilayer number (Figure 4b). The surface coverages were obtained by modeling the frequency change as an increase in mass from a monolayer of 6 nm Au spheres in a face-centered cubic arrangement (volume = 74%). Saturation of the adsorbed amount of DMAP-AuNP occurs at about five PE bilayers (i.e., PEI/PSS/(PAH/PSS)₄ or four PAH/PSS bilayers), giving a surface coverage of about 215 \pm 10% (DMAP-AuNP deposition time for 60 min). These data are in good agreement with the UV-vis experiments. Although the results shown in Figure 4, parts a and b, show that the nanoparticles are infiltrated into the (PAH/PSS)_n multilayer films, as previously reported,³⁵⁻⁴¹ DMAP-AuNP adsorption mainly occurs in the upper region of the PE multilayers. Further, the data suggest that a uniform nanoparticle-nanoparticle distance is maintained, since the DMAP-AuNP adsorbed amounts are essentially saturated above four PAH/PSS bilayers and the λ_{max} position is centered at 600 nm, irrespective of the PE bilayer number (for a constant adsorption time).

In contrast to the PAH/PSS system, PDADMAC/PSS multilayer films show nonsystematic adsorption of DMAP-AuNP. Figure 5 shows the UV-vis spectra of DMAP-AuNP adsorbed onto (PDADMAC/PSS)_n films with increasing bilayer number (*n*) from 1 to 11 for an adsorption time of 60 min. The inset of Figure 5 presents the absorbance of DMAP-AuNP at λ_{max} as a function of film bilayer number. Increasing *n* from 1 to 4 yields an increase in the plasmon absorbance at λ_{max} and causes a red-shift in the absorption peak from 560 (*n* = 1) to 590 nm (*n* = 4). However, further increasing the bilayer number causes a sharp decrease in the plasmon absorbance, which is accompanied by a blue-shift (i.e., λ_{max} = 543 nm for (PDADMAC/PSS)₁₁/DMAP-AuNP). In addition, increasing the DMAP-AuNP adsorption time from 60 to 300 min for the (PDADMAC/PSS)₄ multilayer

(51) Caruso, F.; Lichtenfeld, H.; Donath, E.; Möhwald, H. *Macromolecules* **1999**, *32*, 2317.

(52) Kuo, P. L.; Liang, W. Y.; Wang, F. Y. *J. Polym. Sci. Polym. Chem.* **2003**, *41*, 1360.

(53) Kuo, P. L.; Chen, W. F. *J. Phys. Chem. B* **2003**, *107*, 11267.

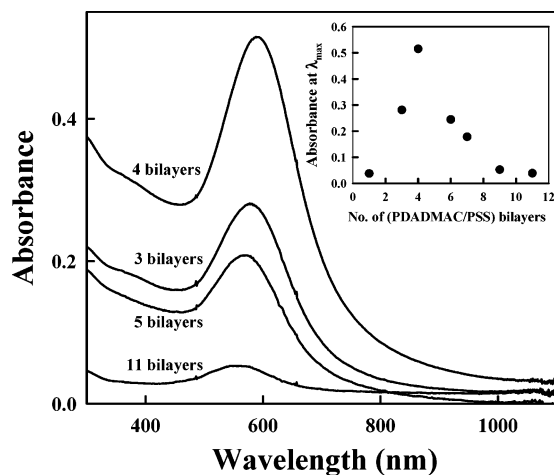


Figure 5. UV-vis absorption spectra of DMAP-AuNP adsorbed onto (PDADMAC/PSS)_n multilayer films with increasing bilayer number. DMAP-AuNP adsorption time = 60 min. Each point in the inset represents the absorbance measured at λ_{max} as a function of PDADMAC/PSS bilayer number.

films results in a monotonic decrease in the adsorbed amount, with no indication of a saturated amount. This is confirmed by QCM measurements (data not shown). The nanoparticle adsorbed amount is also considerably less than for that observed for the PAH/PSS films (compare Figures 4 and 5). These observations are in stark contrast to the trends observed for the PAH/PSS multilayers (see Figure 4). We attribute this adsorption behavior to the excess DMAP in the nanoparticle dispersion. Immersing the PDADMAC/PSS films in 0.1 M DMAP solution (the DMAP-AuNP dispersions contain 0.1 M DMAP) caused disassembly of the films, as observed by the decrease (36%) in absorption peak intensity of PSS (phenyl groups) at 226 nm. At the same time, a new absorption peak due to the pyridine groups of the DMAP ligands at 280 nm was seen (see the Supporting Information). Disassembly of the PDADMAC/PSS films was also confirmed by SPR measurements, which showed a decrease (39%) in film thickness after exposure to 0.1 M DMAP (pH 10.5) solution. As mentioned earlier, PDADMAC does not interact with the DMAP-AuNP. Notably, QCM and SPR experiments show that PAH/PSS multilayer films are also desorbed (38% and 42%, respectively) in the presence of 0.1 M DMAP solution (see the Supporting Information). This is consistent with a report that shows film loss for PAH/PSS multilayers when exposed to pH 10.⁵⁴

The differences in adsorption properties for the PAH/PSS and PDADMAC/PSS films play an important role in the surface morphology of the composite films. DMAP-AuNP were deposited on planar (silicon wafers) and curved (PS particles) substrates precoated with PAH/PSS and PDADMAC/PSS multilayer films. As shown in Figure 6, more dense and uniform coatings are obtained for the PAH/PSS films (Figure 6, parts a and c), compared with the PDADMAC/PSS multilayers (Figure 6, parts b and d).

Based on the above observations, we postulate that when the PAH/PSS multilayers are exposed to the DMAP-AuNP dispersion, the amine groups of PAH deprotonate,⁵⁴ film

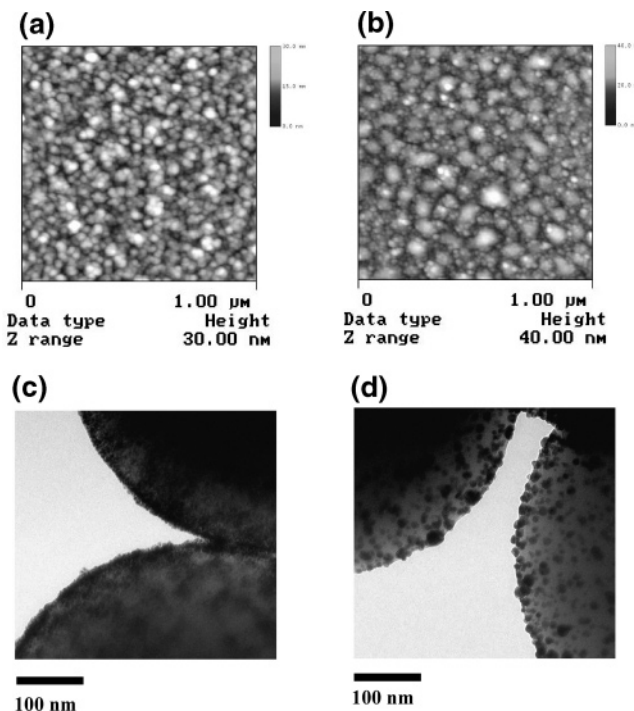


Figure 6. AFM images of (a) (PAH/PSS)₈/DMAP-AuNP and (b) (PDADMAC/PSS)₈/DMAP-AuNP films adsorbed onto a silicon wafer. TEM images of (c) (PAH/PSS)₄/DMAP-AuNP and (d) (PDADMAC/PSS)₄/DMAP-AuNP films adsorbed onto PS colloidal particles of 640 nm diameter.

rearrangement occurs due to a decrease in the electrostatic bonds holding the PAH/PSS layers together,⁵⁴ and the amine groups bond to the gold nanoparticles (DMAP readily desorbs from the nanoparticle surface^{35,43}), while PSS electrostatically associates with the nanoparticles. This effectively results in intra- and interchain “cross-linking” of the films, yielding stable nanoparticle-loaded films. Such a process would only be partially successful for the PDADMAC/PSS films because only PSS interacts with the nanoparticles. Additionally, the large fraction of uncharged DMAP ligands in the nanoparticle dispersion (pH 10.5) may decrease the electrostatic repulsion between DMAP-AuNP (i.e., screen the charges of the nanoparticles) and hence increase the adsorbed amount of DMAP-AuNP onto PAH/PSS-coated substrates. Larson et al. reported that DMAP (1×10^{-3} M at pH 10.5) exists as both neutral (86%) and positively charged species (14%) in aqueous solution.⁵⁵ We further verified that multilayers composed of two components (poly(acrylic acid), PAA, and PAH), both of which associate with the DMAP-AuNP, also result in stable nanoparticle/PE films (data not shown), similar to those observed with PAH/PSS. We are currently exploiting the pH- and temperature-responsive properties of PE multilayers to control the DMAP-AuNP loading and distribution and to modulate the optical properties of the films.

Conclusions

By following the optical properties of DMAP-AuNP, we have shown that in bulk solution, PSS, PAH, and PEI associate with DMAP-AuNP. These interactions can be

(54) Harris, J. J.; DeRose, P. M.; Bruening, M. L. *J. Am. Chem. Soc.* **1999**, *121*, 1978.

(55) Larson, I.; Chan, D. Y. C.; Drummond, C. J.; Grieser, F. *Langmuir* **1997**, *13*, 2429.

exploited for the formation of DMAP–Au_{NP}/PE multilayer films. In the case of PAH/PSS films, stable nanoparticle-loaded multilayer films can be prepared. The adsorption of a dense Au_{NP} coating is driven by the coexisting interactions between the respective PEs (i.e., amine–gold bonding for PAH and electrostatic interaction for PSS) and DMAP–Au_{NP} as well as the large fraction of uncharged DMAP ligand in bulk solution. Infiltration is limited to the surface layers of the PE film, suggesting that the formation of the dense DMAP–Au_{NP} coating in the upper film region prevents the additional adsorption of nanoparticles. Saturated adsorption of DMAP–Au onto PAH/PSS multilayers was achieved for four bilayer PAH/PSS films and for a DMAP–Au_{NP} deposition time of at least 60 min. In contrast, for the multilayer films where PAH is replaced with PDADMAC, a PE that does not associate with the DMAP–Au_{NP}, unstable adsorption behavior is observed for the PDADMAC/PSS multilayers. The PAH/PSS films show a uniform and dense DMAP–Au_{NP} coverage, whereas nonuniform and low nanoparticle coverage was obtained for the PDADMAC/PSS films, despite increasing the nanoparticle adsorption time or increasing the bilayer number for the PDADMAC/PSS films.

Both the amount of DMAP–Au_{NP} adsorbed and the optical properties of the films can be tailored by the number of preassembled PAH/PSS layers (i.e., film thickness). Our findings emphasize the unique adsorption properties induced by polyelectrolyte multilayer films (specifically PAH/PSS) where both components interact with the nanoparticles. Preliminary studies show that the adsorption properties shown by DMAP–Au_{NP} are useful for the preparation of dense nanoparticulate films with other PE multilayers (e.g., PAA and PAH), making these films of general interest in sensing, delivery, or optical applications.

Acknowledgment. This work was supported by the Australian Research Council under the Federation Fellowship and Discovery Project schemes and by the Victorian State Government under the STI Initiative. We thank J. F. Quinn, and A. S. Angelatos for helpful discussions.

Supporting Information Available: UV-vis absorption spectra of multilayer films immersed in 0.1 M DMAP solution. This material is available free of charge via the Internet at <http://pubs.acs.org>.

CM050972B